

First detection of NH_3 ($1_0 \rightarrow 0_0$) from a low mass cloud core^{*,**}

On the low ammonia abundance of the ρ Oph A core

R. Liseau¹, B. Larsson¹, A. Brandeker¹, P. Bergman², P. Bernath³, J. H. Black², R. Booth², V. Buat⁴, C. Curry³, P. Encrenaz⁵, E. Falgarone⁶, P. Feldman⁷, M. Fich³, H. Florén¹, U. Frisk⁸, M. Gerin⁶, E. Gregersen⁹, J. Harju¹⁰, T. Hasegawa¹¹, Å. Hjalmarsen², L. Johansson², S. Kwok¹¹, A. Lecacheux¹², T. Liljeström¹³, K. Mattila¹⁰, G. Mitchell¹⁴, L. Nordh¹⁵, M. Olberg², G. Olofsson¹, L. Pagani⁵, R. Plume¹¹, I. Ristorcelli¹⁶, Aa. Sandqvist¹, F. v. Schéele⁸, G. Serra¹⁶, N. Tothill¹⁴, K. Volk¹¹, and C. Wilson⁹

¹ Stockholm Observatory, SCFAB, Roslagstullsbacken 21, 106 91 Stockholm, Sweden

² Onsala Space Observatory, 439 92 Onsala, Sweden

³ Department of Physics, University of Waterloo, Waterloo, ON N2L 3G1, Canada

⁴ Laboratoire d'Astronomie Spatiale, BP 8, 13376 Marseille Cedex 12, France

⁵ LERMA & FRE 2460 du CNRS, Observatoire de Paris, 61 Av. de l'Observatoire, 75014 Paris, France

⁶ LERMA & FRE 2460 du CNRS, École Normale Supérieure, 24 rue Lhomond, 75005 Paris, France

⁷ Herzberg Institute of Astrophysics, 5071 West Saanich Road, Victoria, BC V9E 2E7, Canada

⁸ Swedish Space Corporation, PO Box 4207, 171 04 Solna, Sweden

⁹ Department of Physics and Astronomy, McMaster University, Hamilton, ON L8S 4M1, Canada

¹⁰ Observatory, PO Box 14, University of Helsinki, 00014 Helsinki, Finland

¹¹ Department of Physics and Astronomy, University of Calgary, Calgary, ABT 2N 1N4, Canada

¹² LESIA, Observatoire de Paris, Section de Meudon, 5 place Jules Janssen, 92195 Meudon Cedex, France

¹³ Metsähovi Radio Observatory, Helsinki University of Technology, Otakaari 5A, 02150 Espoo, Finland

¹⁴ Department of Astronomy and Physics, Saint Mary's University, Halifax, NS B3H 3C3, Canada

¹⁵ Swedish National Space Board, Box 4006, 171 04 Solna, Sweden

¹⁶ CESR, 9 avenue du Colonel Roche, BP 4346, 31029 Toulouse, France

Received 29 November 2002 / Accepted 1 February 2003

Abstract. Odin has successfully observed the molecular core ρ Oph A in the 572.5 GHz rotational ground state line of ammonia, NH_3 ($J_K = 1_0 \rightarrow 0_0$). The interpretation of this result makes use of complementary molecular line data obtained from the ground (C^{17}O and CH_3OH) as part of the Odin preparatory work. Comparison of these observations with theoretical model calculations of line excitation and transfer yields a quite ordinary abundance of methanol, $X(\text{CH}_3\text{OH}) = 3 \times 10^{-9}$. Unless NH_3 is not entirely segregated from C^{17}O and CH_3OH , ammonia is found to be significantly underabundant with respect to typical dense core values, viz. $X(\text{NH}_3) = 8 \times 10^{-10}$.

Key words. ISM: individual objects: ρ Oph A – clouds – molecules – stars: formation

1. Introduction

The ammonia molecule (NH_3) has a complex energy level structure, which makes it a useful tool to probe regions of very different excitation conditions in a given source (see

Send offprint requests to: R. Liseau,
e-mail: rene.liseau@astro.su.se

* Based on observations with Odin, a Swedish-led satellite project funded jointly by the Swedish National Space Board (SNSB), the Canadian Space Agency (CSA), the National Technology Agency of Finland (Tekes) and Centre National d'Études Spatiales (CNES). The Swedish Space Corporation has been the industrial prime contractor.

** and based on observations collected with the Swedish ESO Submillimeter Telescope, SEST, in La Silla, Chile.

Ho & Townes 1983, who also provide an energy level diagram), and molecular clouds have routinely been observed from the ground in the inversion lines at about 1.3 cm, with critical densities of about 10^3 cm^{-3} . On the other hand, the rotational lines have much shorter lifetimes (minutes compared to months) and consequently much higher critical densities ($>10^7 \text{ cm}^{-3}$, see Table 2). Their wavelengths fall, however, into the submillimeter and far infrared regime and these lines are generally not accessible from the ground. Using the Kuiper Airborne Observatory (KAO), the submillimeter ground state line of ammonia of wavelength $524 \mu\text{m}$, NH_3 ($J_K = 1_0 \rightarrow 0_0$), was first and *solely* detected 20 years ago toward Orion OMC1 by Keene et al. (1983). Only recently have renewed attempts been

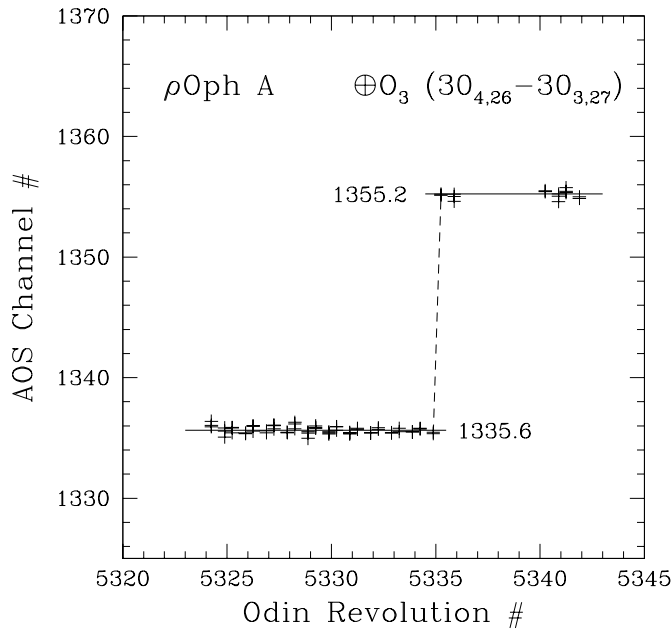


Fig. 1. Gaussian fits to the weak telluric O₃ (30_{4,26}–30_{3,27}) line during the Odin observations of ρ Oph A determined the AOS channel of the line peak (channel width = 0.32 km s⁻¹). The adopted average channel values for the segments, during which the phase lock was stable, are indicated (see the text).

made to observe this line with the spaceborne submillimeter telescope Odin (Frisk et al., Hjalmarsen et al., Larsson et al., Nordh et al. and Olberg et al., this issue).

The cold and dense molecular core ρ Oph A is part of the ρ Ophiuchi cloud at the distance of 160 pc (Loren et al. 1990), which is a region of ongoing low mass star formation. In this Letter, we present Odin observations of ρ Oph A in the NH₃ 572.5 GHz rotational ground state transition. Compared to the KAO, the highly improved sensitivity of Odin permits the clear detection of this tenfold weaker line. These Odin observations were complemented with C¹⁷O and CH₃OH data obtained with the Swedish ESO Submillimeter Telescope (SEST) in La Silla, Chile (see Table 1), aimed at the determination of the average physical conditions of the ρ Oph A core and these are discussed in Sect. 4.1. The Odin observations and their results are presented in Sects. 2 and 3. The implications are discussed, together with our conclusions, in Sect. 4.2.

2. Odin observations and data reductions

Odin observed ρ Oph A in NH₃ on February 13–15, 2002, toward RA = 16^h26^m29^s.78 and Dec = -24° 23' 42".3 (J2000) with a 2' FWHM circular beam. The pointing was accurate to 30", with an rms-stability during these observations better than 5" (Δ RA = \pm 4".7 and Δ Dec = \pm 1".1). The data were obtained in a sky-switching mode (Olberg et al., this issue) by observing a total of 4500 s each ON-source and on blank sky, with 10 s integrations per individual scan. In addition, once per orbital revolution, an OFF-position (1° North) was observed, for a total integration time of 7000 s.

Shortly after launch, it was recognised that the 572 GHz Schottky receiver was not properly phase-locked. However,

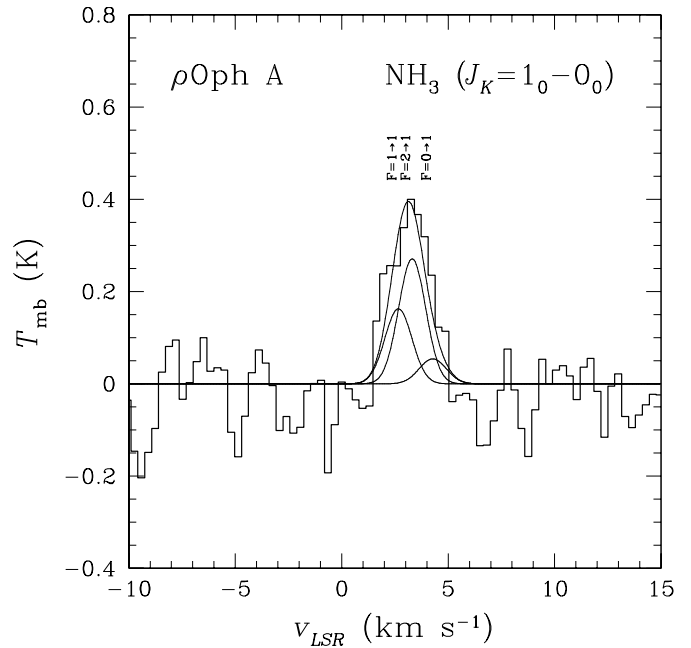


Fig. 2. The submm NH₃ ($J_K = 1_0 - 0_0$) line (523.66 μ m) observed with Odin toward ρ Oph A (histogram). At 572.5 GHz the Odin T_{mb} -scale is related to the flux density by $F_\nu/T_{\text{mb}} = 2600$ Jy/K. The quadrupole hyperfine lines in their equilibrium ratios are indicated, together with their total contribution.

Odin “sees” the Earth’s atmosphere during its revolution and a relatively weak telluric ozone line, O₃ ($J_{K^-,K^+} = 30_{4,26} \rightarrow 30_{3,27}$) 572877.1486 MHz (Pickett et al. 1998), falls sufficiently close to the ammonia line, NH₃ ($J_K = 1_0 \rightarrow 0_0$) 572498.0678 MHz, to allow monitoring of the receiver frequency. For large portions of the ρ Oph A observations, the O₃ line center frequency was within 0.3 of a spectrometer channel (AOS-channel width = 0.32 km s⁻¹) and we used these fiducial channels to restore the remaining data in frequency space (cf. Fig. 1). Data collected during revolution 5336 to 5339 were not used because of too-low mixer current. The reduction procedure is described by Larsson et al. (this issue).

3. Results

The $T_{\text{mb}} = 0.4$ K line ($\eta_{\text{mb}} = 0.9$; Hjalmarsen et al., this issue) of NH₃ (1₀ – 0₀) toward ρ Oph A is centered on $v_{\text{LSR}} = 3.2 \pm 0.1$ km s⁻¹. The width of the hyperfine components (Townes & Schawlow 1955) in Fig. 2 is 1.5 km s⁻¹ and some line broadening results from velocity smearing. In order to discuss the implications of this Odin observation we will first derive the physical characteristics of the source from ground based observations, specifically obtained for the Odin mission. The technical details of these SEST observations will be presented elsewhere.

Table 1. A- and E-state methanol (CH₃OH) observations toward ρ Oph A with the 15 m SEST. η_{mb} and beam-FWHM are, respectively, 0.73 and 52'' for the (2 – 1) and 0.67 and 35'' for the (3 – 2) transitions.

Rotational transition	Frequency ^b (MHz)	E_u/k (K)	$10^6 A_{ul}$ (s ⁻¹)	Observation ^a			CH ₃ OH model		
				v_{LSR} (km s ⁻¹)	Δv (km s ⁻¹)	T_{mb} (K)	T_{R} (K)	τ_0	T_{ex} (K)
2 ₋₁ – 1 ₋₁ E	96739.39	12	2.48		1.51 ± 0.05	0.9 ± 0.1	1.16	-0.07	-11.6
2 ₀ – 1 ₀ A	96741.42	7	2.38		1.52 ± 0.04	1.3 ± 0.1	1.14	0.09	16.3
2 ₀ – 1 ₀ E	96744.58*	20	3.30	3.36 ± 0.09	1.54 ± 0.20	0.3 ± 0.1	0.21	0.05	7.8
2 ₁ – 1 ₁ E	96755.51	28	2.48		0.85 ± 0.31	≤ 0.10	0.04	0.005	11.6
3 ₁ – 2 ₁ A ⁺	143865.79	28	11.16	~0.04 ^c	0.04	0.005	10.2
3 ₀ – 2 ₀ E	145093.75	27	11.93		1.32 ± 0.14	0.50 ± 0.13	0.32	0.04	12.9
3 ₋₁ – 2 ₋₁ E	145097.47*	20	10.61	3.33 ± 0.09	1.53 ± 0.09	1.75 ± 0.06	1.72	0.12	18.4
3 ₀ – 2 ₀ A	145103.23	14	12.23		1.52 ± 0.09	2.15 ± 0.15	2.28	0.21	15.9
3 ₂ – 2 ₂ A ⁻	145124.41	52	6.50			<0.06	0.002	0.0003	9.7
3 ₂ – 2 ₂ E (blend)	145126.37	36	6.63		1.28 ± 0.19	0.25 ± 0.06	0.071	0.009	11.6
3 ₋₂ – 2 ₋₂ E (blend)	145126.37	40	6.63				0.007	0.0004	10.8

Notes:

^a Average of data for two positions, spaced by 30'' North-South.^b Rest frequencies were adopted from Lovas (1992). Tuning frequencies are identified with an asterisk.^c Low resolution spectrum (1.4 MHz). This spectrum includes also DCO⁺ (2 – 1) at a level of $\int T_{\text{mb}} dv_z = 6.4 \text{ K km s}^{-1}$.

4. Discussion and conclusions

4.1. Physical parameters of ρ Oph A

4.1.1. H₂ column density from C¹⁷O ($J = 1 - 0$)

The SEST observations of ρ Oph A in the C¹⁷O (1-0) line (46'' beam, $\eta_{\text{mb}} = 0.70$) revealed spectra with partially resolved hyperfine components. Their relative intensities reflect the ratios of their statistical weights (0.5, 1.0, 0.75), indicating that the levels are populated according to their thermodynamic equilibrium values and that the emission is most likely optically thin. The lines are relatively narrow, $\Delta v = (1.29 \pm 0.05) \text{ km s}^{-1}$, with the main line centered on $v_{\text{LSR}} = (3.41 \pm 0.02) \text{ km s}^{-1}$. From these observations, the beam averaged column density of molecular hydrogen (in cm⁻²) can be estimated from the standard solution of the “radio”-equation of radiative transfer, i.e.

$$N(\text{H}_2) = 2.75 \times 10^{12} \Phi(T_{\text{k}}) \int T_{\text{mb}} dv_z \quad (1)$$

with $\int T_{\text{mb}} dv_z$ in K km s⁻¹ and where

$$\Phi(T_{\text{k}}) = \frac{8\pi k^3 T_{10}^2}{h^3 c^3 g_1 A_{10}} Q(T_{\text{k}}) \frac{\exp(T_{10}/T_{\text{k}})}{1 - J_{\nu}(T_{\text{bg}})/J_{\nu}(T_{\text{k}})}. \quad (2)$$

In Eq. (2), $T_{10} = h\nu_{10}/k = 5.390 \text{ K}$ is the “transition temperature”, $Q(T_{\text{k}}) \sim kT_{\text{k}}/hB$ with $B = 56.1830 \text{ GHz}$ is the partition function, $g_1 = 3$ is the total statistical weight of the upper level $J = 1$, $A_{10} = 7.13 \times 10^{-8} \text{ s}^{-1}$ (Chandra et al. 1996) is the spontaneous transition probability, $T_{\text{bg}} = 2.74 \text{ K}$ is the temperature of the background radiation field and $J_{\nu}(T) = T_{10}/[\exp(T_{10}/T) - 1]$. The numerical constant, $2.75 \times 10^{12} \text{ s cm}^{-3} \text{ K}^{-1}$, assumes the relative abundance of C¹⁷O (with respect to H₂), $X(\text{C}^{17}\text{O}) = 3.6 \times 10^{-8}$, which is consistent with C¹⁸O/C¹⁷O = 4 in ρ Oph A determined by Encrenaz et al. (1973; see also Bensch et al. 2001 for ρ Oph C).

The H₂ column density is not very sensitive to the assumed temperature: the function $\Phi(T_{\text{k}})$ varies within a factor of less than three (2.65) for T_{k} in the range 5 K to 50 K. For the observed line intensity $\int T_{\text{mb}} dv_z = (1.85 \pm 0.06) \text{ K km s}^{-1}$, the H₂ column density is then in the range $(0.5-1.3) \times 10^{23} \text{ cm}^{-2}$. On the arcminute scale, this translates to an average volume density of the order of $n(\text{H}_2) = (0.4-1.0) \times 10^6 \text{ cm}^{-3}$. These results are in accord with earlier molecular line observations (e.g. Loren et al. 1990).

4.1.2. Kinetic gas temperature from CH₃OH ($J = 2 - 1$) and ($J = 3 - 2$)

The observed spectra of 11 CH₃OH lines (Table 1; for an energy level diagram, see Nagai et al. 1979) are suggestive of gas of relatively low excitation (the A⁻ (3₂ – 2₂) line with $E_u/k = 52 \text{ K}$ is not detected and the E (3₂ – 2₂), (3₋₂ – 2₋₂) blend, having $E_u/k \geq 36 \text{ K}$, is weak, if detected at all). We use large velocity gradient models (LVG) of methanol to obtain estimates of the average conditions in the core by requiring acceptable models to be consistent with the C¹⁷O observations.

We consider the rotational J_k energy levels for both A- and E-type methanol in their ground torsional states. The level energies and frequencies were obtained from the JPL-catalogue (Pickett et al. 1998). For the A-states we adopted the Einstein-A values from Pei et al. (1988), whereas we calculated those of the E-states using the equations of Lees (1973), with appropriate Hönl-London factors for the *a*- and *b*-type transitions (e.g. Zare 1986). Rate coefficients for collisions with He were kindly provided by D. Flower (see: Pottage et al. 2001, 2002) and were scaled for collisions with H₂ ($\times 1.37$).

The observed line spectrum (Table 1) is consistent with a model having $T_{\text{k}} = 20 \text{ K}$, $N(\text{H}_2) = 6.0 \times 10^{22} \text{ cm}^{-2}$, $n(\text{H}_2) = 4.5 \times 10^5 \text{ cm}^{-3}$, $dv/dr = 45 \text{ km s}^{-1} \text{ pc}^{-1}$ (1.4 km s^{-1} along 40''),

Table 2. Model results for NH₃ observations toward ρ Oph A.

Transition	NH ₃ model ^a					
	T_{mb} (K)	T_{R} (K)	τ_0	T_{ex} (K)	A_{ul} (s ⁻¹)	$n_{\text{c}}(\text{H}_2)^b$ (cm ⁻³)
o-(1 ₀ - 0 ₀)	0.40	0.41	4.6	6.5	1.59×10^{-3}	3.6×10^7
p-(1 ₁ - 1 ₁) ^c	>0.38	0.88	0.10	11.8	1.69×10^{-7}	2.0×10^3
p-(2 ₂ - 2 ₂) ^c	>0.18	0.23	0.012	21.7	2.26×10^{-7}	2.0×10^3
o-(3 ₃ - 3 ₃)	...	0.04	-0.005	-5.2	2.59×10^{-7}	2.2×10^3

Notes:

^a Ortho-to-para of unity is assumed ($X_{\text{o}}/X_{\text{p}} = 1$).^b Values of the critical density, $n_{\text{c}}(\text{H}_2) = A_{\text{ul}}/C_{\text{ul}}(T_{\text{k}})$, for 20 K.^c Data estimated from Fig. 2 of Zeng et al. (1984) and scaled to the Odin beam size, i.e. multiplied by $(43/120)^2$.

and a methanol abundance of $X(\text{CH}_3\text{OH}) = X_{\text{A}} + X_{\text{E}} = (1.4 + 1.3) \times 10^{-9}$. The model yields thus a ratio $X_{\text{E}}/X_{\text{A}} = 0.89$, which can be compared to the equilibrium ratio of 0.67 at 20 K.

Any beam effects of significance are not evidenced by the CH₃OH data (35'' and 52'' beam sizes), suggestive of emission regions not exceeding half an arcminute. Even the strongest methanol lines have only modest optical depths (max $\tau_0 \leq 0.2$) and the excitation of these lines is only mildly subthermal, giving confidence to our temperature determination. Much higher temperatures (say 50 K) are not consistent with the methanol observations. T_{k} is also equal to the temperature of the *cold* dust component evidenced by ISO-LWS observations (Liseau et al. 1999).

4.2. NH₃ ($J = 1 - 0$) emission from ρ Oph A

The model of the previous sections represents the basis for our analysis of the Odin ammonia line observations, where we varied only the NH₃ abundance. Using the equations of Poynter & Kakar (1975; 15 parameter exponential fit) we computed the level energies and Einstein-A values, with the dipole moment from Cohen & Poynter (1974). The collisional rate coefficients were adopted from Danby et al. (1988).

The observation with Odin (Table 2) can be fit with an ortho-ammonia abundance of, formally, $X_{\text{o}}(\text{NH}_3) = 4.25 \times 10^{-10}$, corresponding to a beam averaged column density $N_{\text{o}}(\text{NH}_3) = 2.6 \times 10^{13} \text{ cm}^{-2}$. ρ Oph A has been mapped in the (1₁-1₁) and (2₂-2₂) inversion lines of NH₃ with the 100 m Effelsberg antenna (43'' beam) by Zeng et al. (1984). Their Fig. 2 displays the spectra toward one position, and the values scaled to the Odin beam size are given in our Table 2, together with our model for an ortho-to-para ratio of unity. According to Zeng et al. (1984), extended ammonia emission on the 90'' scale is also observed. Fortuitously perhaps, a 43'' source (~45'' SE) is also consistent with the (2₂-2₂) and (3₃-3₃) observations by Wootten et al. (1994) with the VLA (6'' beam). The observed and model values are, respectively, 11.5 K and 11.8 K for (2₂-2₂) and 2.2 K and 2.0 K for (3₃-3₃), which is slightly masing. No data are given for their (1₁-1₁) observations, the model value of which is 45.2 K. However, Wootten et al. (1994) used their (1₁-1₁) measurement (in combination

with 2₂-2₂) to estimate $X_{\text{p}}(\text{NH}_3) \sim 3 \times 10^{-10}$. Albeit referring to a much smaller angular scale, this is in reasonable agreement with our ad hoc assumption of equal amounts of ortho- and para-NH₃.

We thus estimate a total ammonia abundance of the order of $X(\text{NH}_3) = 8.5 \times 10^{-10}$ in the ρ Oph A core. This value is significantly lower than the 10^{-8} to 10^{-7} generally quoted for molecular clouds (and cannot be explained by an erroneous ortho-to-para ratio) and contrasts with our value of $X(\text{CH}_3\text{OH})$, which appears entirely “normal” (e.g., van Dishoeck et al. 1993). Although the uniqueness of the present model may be debatable (e.g., gradients in velocity, temperature and density are known to exist over the 2' Odin beam), these results are certainly significant. Smaller velocity gradients, higher temperatures and/or densities would result in even lower $X(\text{NH}_3)$. At the other extreme, “normal” abundances would require the line to be thermalized ($\tau > 10^3$), e.g., at the unrealistically low value of $T_{\text{k}} = 6 \text{ K}$, unless the NH₃ source is point-like. With this caveat in mind, we conclude that the ρ Oph A core likely has a very low NH₃ abundance.

Acknowledgements. We wish to thank the two referees (A. Wootten and one anonymous) for their efforts, which has led to an improvement of the manuscript. We are grateful to D. Flower for providing us with the collision rate constants for methanol.

References

- Bensch, F., Pak, I., Wouterloot, J. G. A., Klapper, G., & Winnewisser, G. 2001, *ApJ*, 562, L185
- Chandra, S., Maheshwari, V. U., & Sharma, A. K. 1996, *A&AS*, 117, 557
- Cohen, E. A., & Poynter, R. L. 1974, *J. Mol. Spec.*, 53, 131
- Danby, G., Flower, D. R., Valiron, P., Schilke, P., & Walmsley, C. M. 1988, *MNRAS*, 235, 229
- Encrenaz, P., Wannier, P. G., Jefferts, K. B., Penzias, A. A., & Wilson, R. W. 1973, *ApJ*, 186, L77
- Ho, P. T. P., & Townes, C. H., 1983, *ARA&A*, 21, 239
- Keene, J., Blake, G. A., & Phillips, T. G. 1983, *ApJ*, 271, L27
- Lees, R. M. 1973, *ApJ*, 184, 763
- Liseau, R., White, G. J., Larsson, B., et al. 1999, *A&A*, 344, 342
- Loren, R. B., Wootten, A., & Wilking, B. A. 1990, *ApJ*, 365, 269
- Lovas, F. J. 1992, *J. Phys. Chem. Ref. Data*, 21, 181
- Nagai, T., Kaifu, N., Nagane, K., & Akabane, K. 1979, *PASJ*, 31, 317
- Pei, C. C., Zeng, Q., & Gou, Q. Q. 1988, *A&AS*, 76, 35
- Pickett, H. M., Poynter, R. L., Cohen, E. A., et al. 1998, *Submillimeter, Millimeter, and Microwave Spectral Line Catalog*, *J. Quant. Spectrosc. & Rad. Transfer*, 60, 883
- Pottage, J. T., Flower, D. R., & Davis, S. L. 2001, *J. Phys. B*, 34, 3313
- Pottage, J. T., Flower, D. R., & Davis, S. L. 2002, *J. Phys. B*, 35, 2541
- Poynter, R. L., & Kakar, R. K. 1975, *ApJS*, 29, 87
- Townes, C. H., & Schawlow, A. L. 1955, *Microwave Spectroscopy* (Dover Publications, Inc.)
- van Dishoeck, E. F., Blake, G. A., Draine, B. T., & Lunine, J. I. 1993, in ed. E. H. Levy, & J. I. Lunine, *Protostars and Planets III* (University of Arizona Press), 163
- Wootten, A., André, P., Despois, D., & Sargent, A. 1994, in *Clouds, Cores and Low Mass Stars*, ed. D. P. Clemens, & R. Barvainis, ASP, 65, 294
- Zare, R. N. 1986, *Angular Momentum* (John Wiley & Sons)
- Zeng, Q., Batrla, W., & Wilson, T. L. 1984, *A&A*, 141, 127